

## Optical Evidence for the Dynamic Jahn-Teller Effect in $\text{Nd}_{0.7}\text{Sr}_{0.3}\text{MnO}_3$

S. G. Kaplan,<sup>1,\*</sup> M. Quijada,<sup>1</sup> H. D. Drew,<sup>1,2</sup> D. B. Tanner,<sup>3</sup> G. C. Xiong,<sup>2</sup> R. Ramesh,<sup>2</sup> C. Kwon,<sup>2</sup> and T. Venkatesan<sup>2</sup>

<sup>1</sup>Laboratory for Physical Sciences, College Park, Maryland 20740

<sup>2</sup>Center for Superconductivity Research, Department of Physics, University of Maryland at College Park, College Park, Maryland 20742

<sup>3</sup>Department of Physics, University of Florida, Gainesville, Florida 32611

(Received 12 February 1996)

The optical properties of  $\text{Nd}_{0.7}\text{Sr}_{0.3}\text{MnO}_3$  thin films have been studied over a broad spectral range, at temperatures down to 15 K and magnetic fields up to 8.9 T. A large transfer of spectral weight from high energy to low energy occurs as this material is cooled into the ferromagnetic phase, or as the magnetic field is increased near the phase boundary. The optical data are found to be consistent with models that include both the double-exchange interaction and the dynamic Jahn-Teller effect on the  $\text{Mn}^{3+} e_g$  levels. [S0031-9007(96)01053-8]

PACS numbers: 75.50.Cc, 78.20.Ls, 78.30.-j

The recent discovery of “colossal” magnetoresistance (CMR) in hole-doped ferromagnetic perovskites of the form  $(Ln)_{1-x}(A)_x\text{MnO}_{3-\delta}$ , where  $Ln$  is a lanthanide and  $A$  is an alkaline-earth element, has revived interest in this complex magnetic system [1]. A decrease in resistance of more than 99% has been observed at temperatures near the Curie point in an applied magnetic field [2]. The observed correlation between the electronic transport and ferromagnetism in this class of materials has been long discussed in terms of an exchange coupling mediated by the electronic hopping between neighboring Mn  $e_g$  orbitals, called the double exchange process [3]. However, it has been pointed out recently [4] that double exchange alone is not sufficient to explain the CMR effect.

On the other hand, it is well known that there is a strong coupling between the electronic and ionic degrees of freedom in these materials. This leads to a static Jahn-Teller (JT) lattice distortion of pure  $\text{LaMnO}_3$  and a magnetic-field induced structural phase transition in  $\text{La}_{0.83}\text{Sr}_{0.17}\text{MnO}_3$  [5]. Although the static JT distortions are not present in the alloys for  $x > 0.2$ , it has been conjectured that dynamic JT effects may be important [6,7]. Indeed this recent theoretical work suggests that the coupling to the lattice leads to a JT small polaron in the paramagnetic state which may be responsible for the high, activated resistivity. In this picture the alignment of the spins in the ferromagnetic state leads to a collapse of the small polaron and a metallic conductivity.

If these new theoretical ideas are correct, there should be an optical signature of the small polarons corresponding to photon induced hopping [8]. However, in a recent optical reflectivity study of  $\text{La}_{0.825}\text{Sr}_{0.175}\text{MnO}_3$  [9], no evidence of Jahn-Teller effects was reported. Instead, the large observed shift in spectral weight from high frequency to low frequency as the sample was cooled into the metallic, ferromagnetic state was interpreted in terms of optical selection rules within the double-exchange picture.

In this paper we present transmittance and reflectance measurements of  $\text{Nd}_{0.7}\text{Sr}_{0.3}\text{MnO}_3$  thin films as a func-

tion of both temperature and magnetic field. Our results also show a large shift in spectral weight from above 1 eV to lower energy as the sample is cooled into the ferromagnetic state. In addition, we observe similar spectral changes as a function of applied magnetic field. These effects demonstrate a broadband change in electronic properties at energies several orders of magnitude larger than either  $\mu_B g H \sim 1$  meV or  $k_B T$ . In contrast to  $\text{La}_{0.825}\text{Sr}_{0.175}\text{MnO}_3$ , however, the optical properties of  $\text{Nd}_{0.7}\text{Sr}_{0.3}\text{MnO}_3$  show evidence for combined double-exchange and dynamic JT effects.

The samples used in this study were  $\text{Nd}_{0.7}\text{Sr}_{0.3}\text{MnO}_3$  thin films grown on  $\text{LaAlO}_3$  and  $\text{Al}_2\text{O}_3$  substrates by pulsed laser deposition in an  $\text{N}_2\text{O}$  atmosphere [2]. The films are epitaxial as revealed by x-ray diffraction, and show 3 MeV  $\text{He}^+$  ion Rutherford backscattering channeling spectra with a minimum yield of 3.8%, indicating a high degree of crystallinity. For the sample discussed below, grown on an  $\text{Al}_2\text{O}_3$  substrate, the room temperature dc resistivity measured with a four-probe method was  $2 \times 10^{-3} \Omega \text{ m}$ . The maximum resistivity, at 180 K, was  $2.4 \times 10^{-2} \Omega \text{ m}$ .

Transmittance and reflectance measurements were performed with a combination of Fourier transform spectrometers and grating monochromators to cover the investigated regions of 5 to 25 meV and 0.25 to 3 eV. High magnetic field transmittance measurements in the Faraday geometry were made with a 9 T superconducting solenoid, using either a lightpipe or optical fiber to gain access to the bore of the magnet. The combined relative uncertainty in the absolute transmittance is  $\pm 5\%$  from 5 to 25 meV and  $\pm 8\%$  from 0.25 to 3 eV. (Two standard deviations are used in reporting uncertainties in this paper.) The relative uncertainty in the reflectance spectra is estimated at  $\pm 6\%$ .

Transmittance and reflectance spectra at zero magnetic field from 15 to 300 K for a  $140 \pm 10$  nm thick  $\text{Nd}_{0.7}\text{Sr}_{0.3}\text{MnO}_3$  film on a 0.5 mm thick  $\text{Al}_2\text{O}_3$  substrate are shown in Fig. 1. The inset in Fig. 1(b) shows the low frequency transmittance of this film from 15 to 240 K,

relative to a blank  $\text{Al}_2\text{O}_3$  substrate. The free-carrier absorption is very weak in this sample, which is clear from the strong phonon feature that appears at 21 meV. Since the low-frequency transmittance of the film is different from 1 by less than  $\sim 35\%$ , we can expand the standard sheet conductance formula to linear terms in conductivity,  $\sigma$ , and find that

$$T_{FS}/T_S \approx 1 - 2Z_0\sigma_1d/(n+1). \quad (1)$$

Here  $T_{FS}$  and  $T_S$  are the transmittance of the film/substrate and substrate, respectively,  $n = 3.5$  is the index of refraction of the substrate,  $d$  is the film thickness,  $\sigma_1$  is the real part of the film conductivity, and  $Z_0$  is the impedance of free space. Thus, the low-frequency conductivity can be obtained directly from the low frequency transmittance values.

The room temperature conductivity at 5 meV is approximately 10 times larger than the measured dc value of this sample, indicative of the granular nature of the conductance in this type of thin film material [10]. The 5 meV conductivity has a minimum as a function of temperature at 180 K, showing the same trend as the dc conductivity. Similar behavior has been found for the microwave conductivity of these materials [11]. Also, the conductivity increases as a function of frequency, in contrast to a simple free-carrier response.

The conductivity from 0.25 to 3 eV is obtained from the transmittance and reflectance curves shown in Fig. 1 by numerically inverting the exact Fresnel formulas for a thin film on a thick substrate. The combined uncertainty in the derived conductivity values, which is dominated by the uncertainty in the film thickness, is  $\pm 20\%$ .

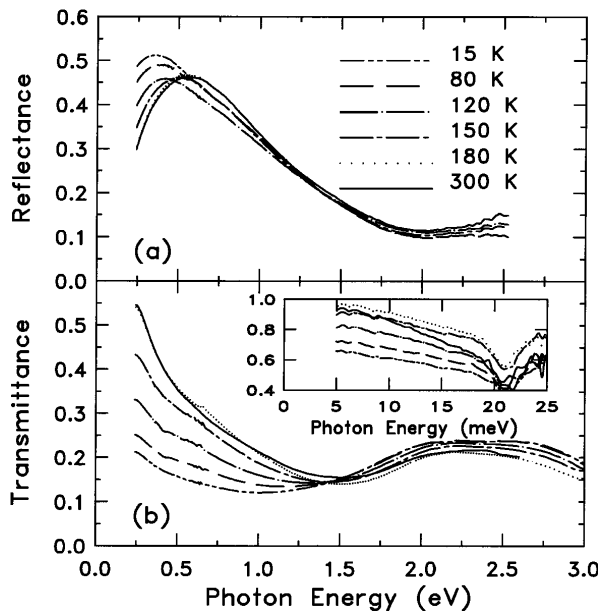


FIG. 1. Reflectance (a) and transmittance (b) of a 140 nm thick  $\text{Nd}_{0.7}\text{Sr}_{0.3}\text{MnO}_3$  film on  $\text{Al}_2\text{O}_3$  at zero magnetic field for various temperatures. The inset in (b) shows the FIR transmittance, in this case the solid line is the transmittance at 240 rather than 300 K.

The real part of the optical conductivity at zero field derived from the data in Fig. 1 is shown in Fig. 2. The symbols near the origin show the conductivity at 5 meV, while the solid and dashed curves show the conductivity derived from the high-frequency transmittance and reflectance data. The room temperature curve shows an absorption band centered near 1.2 eV, and the beginning of another band beyond the high energy limit of the data. As the temperature is lowered below 180 K, the conductivity at lower energy increases dramatically, while decreasing somewhat at higher energy. At the same time, the peak in the conductivity shifts to lower energy and broadens.

A comparison of the temperature dependence and the magnetic-field dependence of the transmittance is shown in Fig. 3. Figure 3(a) shows the ratio of the transmittance at a given temperature to that at 180 K, for temperatures below 180 K, and Fig. 3(b) the ratio of transmittance at 8.9 T to that at 0 T over the same temperature range. A striking similarity can be seen between Figs. 3(a) and 3(b), indicating that the spectral changes upon decreasing the temperature relative to 180 K, or upon increasing the applied field at a given temperature, are due to the charges in spin alignment.

The peak in the magnetotransmittance effect is at 180 K, the same temperature as the peak in the dc and 5 meV resistivities. The magnetic-field decreases at both lower and higher temperatures, decreasing to about half the peak value by 240 K, and 20% of the peak value by 15 K. The fact that a significant magnetic field dependence persists in this sample down to the lowest measured temperature is an indication of magnetic disorder in the film (or, possibly, of a cantered ferromagnetic ground state) as noted by others [11–13].

To make a more quantitative comparison between the magnetic-field and temperature dependence of the optical

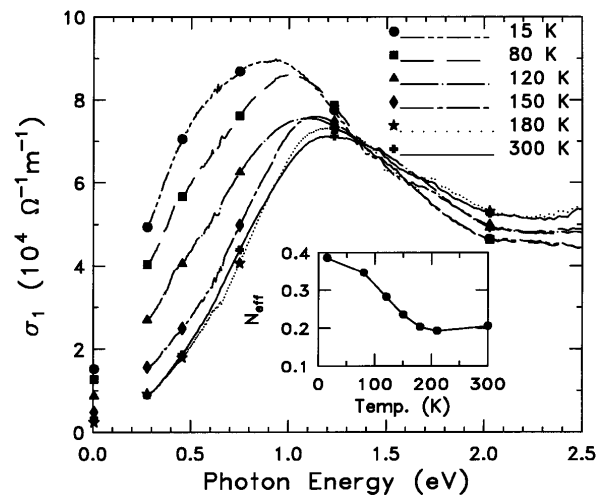


FIG. 2. Real part of the optical conductivity,  $\sigma_1$ , versus photon energy derived from the data in Fig. 1. A large transfer of spectral weight from high to low energy is apparent, along with a shift in the peak to lower energy as the temperature is decreased. Inset:  $N_{\text{eff}}$  integrated up to 1.5 eV versus temperature.

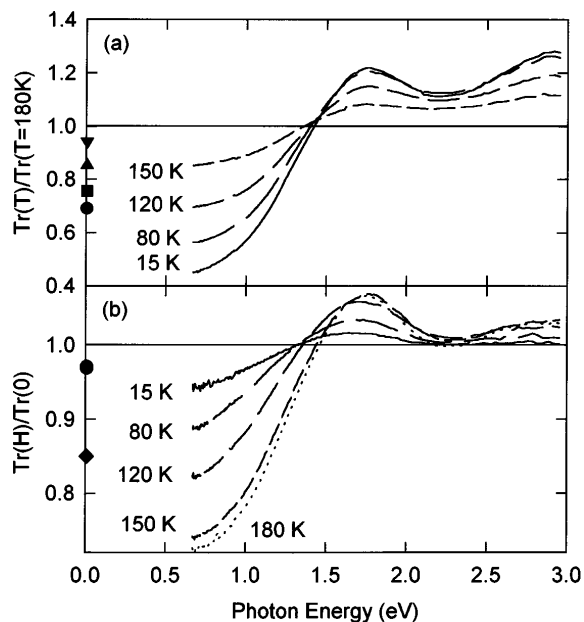


FIG. 3. Transmittance ratios for temperature (a) and magnetic field (b) for the 140 nm  $\text{Nd}_{0.7}\text{Sr}_{0.3}\text{MnO}_3$  sample. Frame (a) shows the ratio of the transmittance at several temperatures to that at 180 K at zero field, while (b) shows the ratio for  $H = 8.9$  to 0 T at 180 K and below. In frame (b), the solid circle shows the FIR transmittance ratio at 15 K, and the diamond the ratio at 150 K.

conductivity, we fit the conductivity at zero field with a sum of a Drude and Lorentzian terms, and use this fit as a basis for fitting the high-field transmittance. The Drude term, which is required to describe the low-frequency limit, is weak and the fits are insensitive to its width. These results are shown in Fig. 4(a) as the fitted change in  $\sigma_1$  at 180 K between 8.9 and 0 T, compared to the difference between the measured zero-field  $\sigma_1$  at 15 and 180 K, in Fig. 4(b). The similarity of the two curves reaffirms the conclusion that the changes in conductivity induced by lowering the temperature or raising the magnetic field are driven by the spin polarization of the system.

The qualitative effect of transfer of oscillator strength from high frequency to low frequency as a function of spin polarization appears to be characteristic of CMR manganites; we have found a magneto-optical response very similar to that shown in Fig. 3(b) in a  $\text{La}_{0.7}\text{Ba}_{0.3}\text{MnO}_3$  film at 240 K. This sample has a measured dc resistivity about 2 orders of magnitude smaller than the  $\text{Nd}_{0.7}\text{Sr}_{0.3}\text{MnO}_3$  film, and shows almost no magneto-optic response at low temperature, consistent with nearly saturated ferromagnet.

In the inset to Fig. 2 we show the temperature dependence of the oscillator strength expressed in terms of the effective electron density

$$N_{\text{eff}}(\omega) = \frac{2V_{\text{cell}}m}{\pi e^2} \int \sigma_1(\omega') d\omega', \quad (2)$$

integrated to 1.5 eV (where  $\Delta\sigma \cong 0$ ).  $V_{\text{eff}}$  is the unit cell volume. It is apparent from both Figs. 2 and 4 that the oscillator strength sum rule is not satisfied over

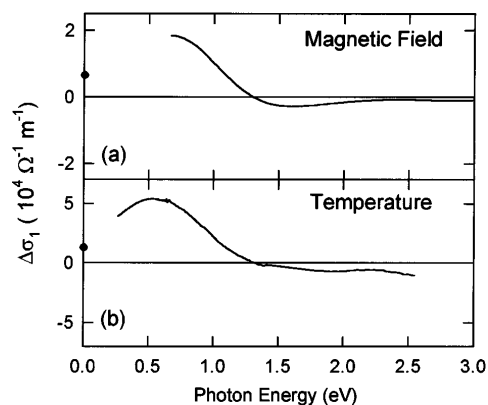


FIG. 4. Comparison of (a) the fitted difference  $\Delta\sigma_1 = \sigma_1(180 \text{ K}, 8.9 \text{ T}) - \sigma_1(180 \text{ K}, 0 \text{ T})$  with (b) the measured difference  $\Delta\sigma_1 = \sigma_1(15 \text{ K}, 0 \text{ T}) - \sigma_1(180 \text{ K}, 0 \text{ T})$ . The change in spectral weight has a similar shape in both cases, with the large increase at low energy implying that the decrease above 1.2 eV must extend to higher energy.

the range of photon energies that we have investigated. As the temperature is lowered, the oscillator strength above 1.5 eV decreases, but more slowly than the growth at lower frequency (and more slowly than is found in  $\text{La}_{0.825}\text{Sr}_{0.175}\text{MnO}_3$  [9]). Thus, the magnetic-field and temperature dependence must extend to higher energies.

Now we turn to the interpretation of these optical data. The conductivity of pure  $\text{LaMnO}_3$  in the vicinity of 1 eV is negligibly small [14]. The behavior of  $\text{NdMnO}_3$  is expected to be similar. Since the Sr doping introduces holes in the Mn  $e_g$ -derived levels, the peak in the alloy conductivity near 1 eV must involve these Mn  $e_g$  levels. The increase of the spectral weight of this peak as the temperature is lowered below  $T_c$  shows that this feature cannot be due simply to onsite  $d-d$  transitions between spin-split Mn  $e_g$  levels, since such transitions would be insensitive to relative alignment of adjacent core ( $t_{2g}$ ) spins. On the other hand, its strong temperature and magnetic-field dependence implies that it must involve the  $e_g$ -derived states in an important way. Indeed, both the initial and final states must have a large  $e_g$  component. If, for example, the absorption peak was due to transitions from the  $\text{O}(2p)$  states to the  $e_g$  derived states, then both  $\text{O}(2p)$  spins would participate, and the transition would not depend on the orientation of the Mn core spins. Thus, the main component of the conductivity peak must be a charge transfer transition between Mn  $e_g$ -derived levels of adjacent sites. For the case where the final state is on an already occupied site (as in  $\text{LaMnO}_3$ ), the transition energy would be shifted to well above the investigated region by the on-site Coulomb energy  $U \sim 4$  eV. Therefore, we conclude that the absorption must be due to a charge transfer transition from a  $\text{Mn}^{3+} e_g$  level to the unoccupied  $\text{Mn}^{4+} e_g$  levels on an adjacent site [15]. This transition is mediated by the hopping matrix element which is also responsible for the metallic conductivity in the ferromagnetic state. Since the dc conductivity in these materials can be very high, a sizable

optical matrix element is not unreasonable. It is, however, appreciably weaker than typical  $d \rightarrow sp$  charge transfer transitions observed in other transition metal oxides such as  $\text{LiNbO}_3$  and  $\text{TiO}_2$  [16].

Millis, Mueller, and Shraiman [15] suggest that this conductivity peak is to be interpreted as the transition from a lower dynamic Jahn-Teller split  $\text{Mn}^{3+} e_g$  level to the unsplit  $\text{Mn}^{4+} e_g$  levels of a neighboring site. In their model, which includes both double-exchange and JT polaron effects, the JT splitting collapses when the ratio,  $\lambda^2$ , of the Jahn-Teller self-trapping energy to the  $e_g$  bandwidth falls below a critical value [7,17]. The  $e_g$  bandwidth depends on the spin alignment through the double-exchange driven hopping probability. The optical transition energy in the ferromagnetic state is expected to be larger than half of the JT splitting because of the difference between the centers of gravity of the  $e_g$  levels on the  $\text{Mn}^{4+}$  and  $\text{Mn}^{3+}$  ions. Optical conductivity curves calculated within this model show shifts in oscillator strength, linewidth, and peak position versus temperature, which are similar to the data in Fig. 2 [17].

Optical transitions involving  $O(2p)$  orbitals may also be expected in this spectral range, as indicated by others [9,12]. Therefore, the 1.2 eV peak in Fig. 2 could contain contributions from several optical transitions. However, as argued above, these other transitions would not contribute to the observed temperature and magnetic field dependence. Additional measurements and systematic doping studies will be required to apportion the various contributions to the optical conductivity.

It is interesting to consider the published data on  $\text{La}_{0.825}\text{Sr}_{0.175}\text{MnO}_3$  within the double-exchange and JT polaron model. At room temperature, the conductivity has a broad peak near 1 eV, which collapses to a nearly frequency independent conductivity up to 2.5 eV in the ferromagnetic state. In the optical conductivity calculations of Millis *et al.* [17], this behavior is obtained for small values of  $\lambda^2$ . Therefore, it appears that the difference in the low temperature behavior of the transport and optical properties of the two materials can be understood in terms of a finite JT gap in  $\text{Nd}_{0.7}\text{Sr}_{0.3}\text{MnO}_3$  and a near zero gap in  $\text{La}_{0.825}\text{Sr}_{0.175}\text{MnO}_3$ . The smaller size of the Nd ion, compared to the La ion, leads to greater Mn-O-Mn bond angle distortions, so that a stronger JT coupling and a larger JT gap is expected for  $\text{Nd}_{0.7}\text{Sr}_{0.3}\text{MnO}_3$  [18]. The larger JT gap for  $\text{Nd}_{0.7}\text{Sr}_{0.3}\text{MnO}_3$  is also suggested by the fact that the sum rule is not satisfied over the measured range.

In summary, we have found the optical conductivity of  $\text{Nd}_{0.7}\text{Sr}_{0.3}\text{MnO}_3$  in the range 0 to 2.5 eV to be dominated by a broad peak near 1.2 eV at room temperature. The spin-polarization dependence of this absorption band leads us to assign it to an  $\text{Mn}^{3+}$  to  $\text{Mn}^{4+}$  charge transfer transition. The temperature dependence of the conductivity spectrum is found to be remarkably similar to model calculations in which the double-exchange driven hopping is coupled to dynamic Jahn-Teller polaron effects.

We would like to thank R. Liu, J.P. Rice, and R.U. Datla for use of their optical magnet cryostat system at NIST in the early stages of this work. We would also like to thank A.J. Millis for communicating the results of the model discussed in the text to us prior to publication. In addition, we acknowledge useful discussions with S.M. Bhagat, S.E. Lofland, S. Wu, E-J. Choi, R.L. Greene, K.L. Empson, R.S. Decca, and V. Kostur. Work performed in affiliation with the NSF-MRSEC DMR-96-32521.

\*Current address: Optical Technology Division, National Institute of Standards and Technology, Gaithersburg, MD 20899.

- [1] R. M. Kusters, J. Singleton, D. A. Keen, R. Mcgreevy, and W. Hayes, *Physica B* **155**, 362 (1989); R. Von Helmolt, J. Wecker, B. Holzapfel, L. Schultz, and K. Samwer, *Phys. Rev. Lett.* **71**, 2331 (1993); K. I. Chahara, T. Ohno, M. Kasai, and Y. Kozono, *Appl. Phys. Lett.* **63**, 1990 (1993); S. Jin, T. H. Tiefel, M. McCormack, R. A. Fastnacht, R. Ramesh, and L. H. Chen, *Science* **264**, 413 (1994); M. McCormack, S. Jin, T. H. Tiefel, R. M. Fleming, J. M. Phillips, and R. Ramesh, *Appl. Phys. Lett.* **64**, 3407 (1994); H. L. Ju, C. Kwon, Q. Li, R. L. Greene, and T. Venkatesan, *Appl. Phys. Lett.* **65**, 2109 (1994).
- [2] G. C. Xiong, Q. Li, H. L. Ju, S. N. Mao, L. Senapati, X. X. Xi, R. L. Greene, and T. Venkatesan, *Appl. Phys. Lett.* **66**, 1427 (1995).
- [3] C. Zener, *Phys. Rev. B* **82**, 403 (1951); P. W. Anderson and H. Hasegawa, *Phys. Rev.* **100**, 675 (1955); P.-G. de Gennes, *Phys. Rev.* **118**, 141 (1960).
- [4] A. J. Millis, P. B. Littlewood, and B. I. Shraiman, *Phys. Rev. Lett.* **74**, 5144 (1995).
- [5] A. Asamitsu, Y. Moritomo, Y. Tomioka, T. Arima, and Y. Tokura, *Nature (London)* **373**, 407 (1995).
- [6] H. Röder, Jun Zang, and A. R. Bishop, *Phys. Rev. Lett.* **76**, 1356 (1996).
- [7] A. J. Millis, Boris I. Shraiman, and R. Mueller, *Phys. Rev. Lett.* **77**, 175 (1996).
- [8] G. D. Mahan, *Many-Particle Physics* (Plenum Press, New York, 1981), Chap. 6.
- [9] Y. Okimoto, T. Katsufuji, T. Ishikawa, A. Urushibara, T. Arima, and Y. Tokura, *Phys. Rev. Lett.* **75**, 109 (1995).
- [10] This effect is sample dependent. In films grown on  $\text{LaAlO}_3$  substrates the FIR and dc conductivities are in better agreement while the optical response at room temperature is nearly identical to the results reported in this paper.
- [11] Dominguez *et al.*, *Europhys. Lett.* **32**, 349 (1995).
- [12] J. F. Lawler, J. G. Lunney, and J. M. D. Coey, *Appl. Phys. Lett.* **65**, 3017 (1994).
- [13] J. M. D. Coey, M. Viret, L. Ranno, and K. Ounadjela, *Phys. Rev. Lett.* **75**, 3910 (1995).
- [14] T. Arima, Y. Tokura, and J. B. Torrance, *Phys. Rev. B* **48**, 17006 (1993).
- [15] A. J. Millis, private communication (1996).
- [16] *Handbook of Optical Constants*, edited by E. D. Palik (Academic, New York, 1985).
- [17] A. J. Millis, R. Mueller, and Boris I. Shraiman, *Phys. Rev. B* (to be published).
- [18] H. Hwang *et al.*, *Phys. Rev. Lett.* **75**, 914 (1995).